Article

Methane Production Reduced by Lignin Derivatives in Pulping Wastewater: Inhibition of Free Hydrolase

Jinxu Lei [1], Zhihong Xu [1], Yong Chen [1], Guo Yu [1], Zexiang Liu [1], Shuangfei Wang [1,2,*], Jian Zhang [1,2,3,*], Kelin Li [1] and Li Xie [1]

1 Guangxi Key Laboratory of Clean Pulp & Papermaking and Pollution Control, College of Light Industry and Food Engineering, Guangxi University, Nanning 530004, China; jiubaby999@163.com (J.L.)
2 Guangxi Bossco Environmental Protection Technology Co., Ltd., Nanning 530007, China
3 Provincial and Ministerial Collaborative Innovation Center for Sugar Industry, Nanning 530004, China
* Correspondence: wangsf@gxu.edu.cn (S.W.); zhangjian_gx@gxu.edu.cn (J.Z.)

Abstract: The lignin derivatives generated during pulping might be responsible for the suboptimal performance of anaerobic reactors during the treatment of pulping wastewater. However, the exact mechanisms by which these derivatives exert influence remain unclear. This study investigated the influence of lignin derivatives, simulated using humic acids (HAs), in anaerobic granular sludge (AnGS). Compared to the enzymes present during floc-bonding and granule-bonding, the HAs impeded the conversion of unhydrolyzed substrates into methane and caused considerable inactivation of free enzymes. Simultaneously, the HAs suppressed agglomeration and weakened the strength of the AnGS. Furthermore, calcium ions helped maintain the integrity of the sludge structure. Therefore, the inhibition of extracellular enzymes using lignin derivatives delays the methanation of unhydrolyzed substrates, resulting in a reduced biomass within AnGS reactors owing to sludge disintegration and biomass loss. This study serves as a reference for investigating the persistent risks originating from lignin derivatives associated with using anaerobic granular-sludge bed reactors to treat pulping wastewater.

Keywords: granule sludge; anaerobic digestion; enzyme; humic acids; pulping wastewater

1. Introduction

Pulping wastewater contains abundant organic matter originating from plant materials (such as wood, straw, and bamboo) released during pulping [1,2]. The liquid waste generated from chemical pulping, often referred to as "black liquor", undergoes an evaporation–concentration–alkali-recovery process [3–5]. This treatment aims to recover chemicals and energy while preventing the entry of lignin derivatives, which are difficult to degrade in wastewater treatment systems [6,7]. Chemical thermomechanical pulp (CTMP, a high-yield pulp) integrates chemical impregnation and mechanical disintegration to extract plant fibers, achieving a yield of 82% to 90%. This exceeds that of chemical pulp, which typically yields less than 50% [8,9]. Recently, China has considerably enhanced its ability to produce CTMP to compensate for the shortage of paper fibers due to the disruption of waste paper import. The liquid waste from CTMP has a notably lower concentration of organic matter compared to black liquor generated through chemical pulping [10–12]. This discrepancy leads to substantial energy consumption during evaporation and concentration [13,14], which, in turn, compromises the efficiency of evaporation–concentration–alkali-recovery treatment. Consequently, anaerobic–aerobic–deep-oxidation is the standard procedure used to manage CTMP effluents. Biological methods, particularly anaerobic digestion, are crucial for eliminating degradable organic matter from wastewater [15,16]. Anaerobic digestion is the most suitable method for treating pulp and paper wastewater as well as for maximizing resource utilization, owing to its advantages of low energy consumption, a high load capacity, and efficient energy recovery. Wood extractives (substances extracted

from wood during pulping), volatile organic acids, lignin, and other organic materials are abundant in CTMP wastewater. Although a few studies [17–19] have demonstrated that lignin derivatives formed by lignin leaching or degradation may exert a unique inhibition effect on pulp and paper wastewater [20,21], the mechanisms by which lignin derivatives function in the anaerobic treatment of CTMP wastewater remain unknown.

Hydrolysis and acidification are prerequisites for the complete decomposition and conversion of organic molecules into methane. The extracellular hydrolysis of organic substrates occurring outside cells enhances the solubility of the substrates and reduces their molecular weight, thereby facilitating the penetration of the cell wall [22–24]. Enzymes may exist in anaerobic granular sludge (AnGS) bed reactors in three distinct forms: free, floc-bound, or granule-bound. The presence of extracellular enzymes in the floc-bound or granule-bound states is crucial for maintaining their activity, as flocculated or granular sludge prevents the deactivation of enzymes. Therefore, considering the occurrence forms of enzymes is essential [25]. Furthermore, changes in the size or spatial arrangement of a substrate caused by lignin derivatives influence the ability of extracellular enzymes to interact with the substrate, thereby decreasing the efficiency of anaerobic digestion [26].

Humic acids (HAs) and lignin have common functional groups, including phenols, quinones, ketones, and carboxyls [27], while lignin derivatives are essential precursors of HAs [28]. Therefore, HAs can serve as model substances for lignin derivatives in CTMP wastewater when investigating the effects and mechanisms of lignin derivatives on the anaerobic treatment of CTMP wastewater. HAs are inactive during digestion, which complicates decomposition and conversion [29]. HAs impede the activity of enzymes that break down organic matter and disrupt sludge granules [30]. Substances and enzymes that are free from the cell will bind to HAs and alter the solubility of substances. In addition, the morphology of enzymes delays the breakdown of substances or inhibits methanogenic activity [31–33]. Moreover, HAs can serve as electron carriers that enhance the transfer of electrons between different species, thereby sustaining anaerobic digestion [14] or altering the accumulation of intermediate products [15,16]. Therefore, further investigations are required to determine the role of lignin derivatives in the anaerobic treatment of wastewater. Calcium ions (Ca ions) are abundant (600–1000 mg/L) in the wastewater generated by pulp and paper mills [34]. The source of the Ca ions was found to be the high Ca ion concentration (600–2500 mg/L) in the white water of a paper machine in which the ions were produced using light calcium carbonate and other auxiliary materials during papermaking [35]. To mitigate potential toxicity, the wastewater from CTMP is typically mixed and diluted with white water from paper machines before anaerobic treatment [36]. Therefore, this study introduced Ca ions in simulation experiments to better simulate the actual situation. HAs possess a negative charge and exhibit abundant carboxyl groups on their surface, making them prone to mutual binding with Ca ions via electrostatic interactions [37,38]. Ca ions are essential for the formation of flocs and the granularity of sludge. Additionally, interactions between lignin derivatives and Ca ions may alter the structure and the trend of granularity of sludge [39]. Hence, the presence of Ca ions should be duly considered as an important factor when investigating the inhibition of lignin derivatives in CTMP wastewater.

Therefore, this study aimed to explore the influence mechanism of lignin derivatives in CTMP wastewater from two perspectives: the occurrence forms of enzymes and the structure of AnGS. Sequential batch experiments were conducted using HAs as a representative model for lignin derivatives. Moreover, the impact of AnGS on the degradation of different substrates (starch, casein, glucose, and sodium acetate) was investigated using varying degrees of hydrolysis in simulated pulping wastewater (with an HA concentration of 3 g/L). Moreover, the effects of HAs on sludge flocculation behavior and the possibility for hydrolysis to occur were assessed by analyzing enzymatic activity and the structure of sludge. In addition, the influence of Ca ions in CTMP wastewater was characterized according to the electrostatic repulsion force and the granularity of sludge. Finally, the occurrence

of different enzymes was used to determine the main mechanism of the interaction with lignin derivatives.

2. Materials and Methods

2.1. Inoculum Preparation

Granular sludge with particle sizes of 0.3–3 mm and total suspended solids/volatile suspended solids (TSS/VSS) not less than 0.7 was harvested from a typical paper mill in Guangxi, China. The granular sludge was treated using ultrasonication to imitate flocculent sludge (20 kHz, 1 W/mL, 20 min). Both flocculated and granular sludge were cultivated in 250 mL fermentation flasks for roughly one week, with the simulated wastewater having a chemical oxygen demand (COD) of 8000 mg/L. The carbon sources used were glucose (Tianjin Zhiyuan Chemical Reagent Co, Tianjin, China) and sodium acetate (Tianjin Zhiyuan Chemical Reagent Co, Tianjin, China), used at an acidification value (i.e., the ratio of the COD of glucose to the COD of sodium acetate) of 50%. To ensure that the activated sludge would perform its normal physiological functions, each fermentation flask was incubated in a water bath (35 ± 0.5 °C, 105 rpm) daily. The substrate was substituted at a predetermined time every day. After filtration using a strainer, the wastewater was mixed with the freshly produced simulated wastewater.

2.2. Chemical Analysis

VFAs (volatile fatty acids) were measured using gas chromatography (GC8890A, Agilent Technologies, Palo Alto, CA, USA) and a hydrogen flame ionization detector. The measurements were performed using a polar column type HP-INNOWAX (Agilent, Santa Clara, CA, USA) with dimensions of 30 m × 0.25 mm × 0.25 μm. The specimens were introduced into the injection port at a split ratio of 1:1. The injection volume was 1.0 μL and the carrier gas used was Nitrogen (N_2) flowing at a rate of 40 mL/min. The temperature program was as follows: the initial column temperature was set to 80 °C, which was raised to 110 °C at a rate of 20 °C per minute and then finally increased to 220 °C at a rate of 10 °C per minute. The temperature was maintained at 220 °C for 2 min. The entire procedure lasted 16.5 min. The temperatures of the input and detector were adjusted to 250 °C. COD was determined using the rapid digestion method with a COD digester (model 5B-3C, Beijing Lianhuayongxing Technology Co., Ltd., Beijing, China). TSS/VSS was measured according to CJ/T 221-2005 [40].

2.3. Granule Disintegration

An experiment performed using 250 mL serum bottles was used to determine how HAs and Ca ions individually influence the structure and granularity of sludge in different forms. Each group contained 20 mL of floc sludge and 100 mL of simulated wastewater. The simulated wastewater contained sodium acetate, glucose, and trace elements. Commercial HAs (3 g/L; CAS 1415-93-6; Shanghai Aladdin Co., Ltd., Shanghai, China) were added to the HA group. A HA–Ca group was treated using 3 g/L HAs and 250 mg/L of Ca ion solutions. Meanwhile, a CA group was added to a 250-mg/L Ca ion solution. A blank group was prepared using simulated wastewater containing sodium acetate and glucose (3000 mg/L COD) as substrates. Samples were collected at 1, 6, 12, 36, and 60 h after the tests began. The experiments were conducted at 35 ± 0.5 °C and utilized a water bath at 80 rpm. A laser particle-size analyzer (Bettersize 2600, Dandong Batter Instrument Co., Ltd., Dandong, China) was used to measure the particle size distribution of the flocculated sludge (D10, D50, D90, and 10th–50th–90th percentile of a particle-diameter distribution curve). The granular sludge was separated into four groups: blank, HA, HA–Ca, and CA groups. Distilled water was used instead of simulated wastewater, and the four groups were incubated for 60 h at 35 ± 0.5 °C in a water bath at 80 rpm before being tested to determine the extracellular polymer substances (EPSs) present. All experiments were performed in duplicate.

2.4. EPS Extraction and Characterization

EPSs are polymers found external to the cells in anaerobic digestion sludge and play a crucial role in material exchange [41]. EPSs are mainly composed of proteins (PNs) and polysaccharides (PSs), which together usually represent the content of EPS. The extraction of EPSs was conducted as follows: 5 g of sludge was rinsed three times using a 0.01-mol/L phosphate-buffered solution), 15 mL of the same solution was added, and then the mixture was centrifuged at 3200 r/min for 30 min. The supernatant was discarded. After adding 15 mL of a 0.85% NaCl solution to the sediment, the mixture was centrifuged for 20 min at 8000 rpm to obtain loosely bound extracellular polymeric substances (LB-EPSs). After adding 15 mL of a 0.85% NaCl solution to the sediment in a water bath at 80 °C for 30 min, tightly bound extracellular polymeric substances (TB-EPSs) were obtained as the supernatant by centrifuging the mixture at 3200 r/min. LB-EPS and TB-EPS extracts were filtered over a 0.45 μm hydrophilic polyethersulfone (PES) membrane filter. The PN content was determined using the modified Folin–Lowry method [42], while the PS content was analyzed using the Anthrone method [43].

2.5. Zeta Potential

After different treatments, the zeta potentials of the original granular sludge, flocculated sludge, 3 g/L of the HA solution, 5 mL of the sludge mentioned above, and substrate samples were measured using a nanoparticle sizer (Nano-ZS90X Zeta, Malvern Panaco Ltd., Malvern, UK). The pH values of the sample solutions were simultaneously measured. The above experiments were conducted in triplicates.

2.6. Total Organic Carbon of Substrate

To investigate the impact of HAs and Ca ions on the total organic carbon (TOC) of substrates in the solutions, two distinct substrates (starch and casein) were treated using HAs, HAs + Ca ions, and Ca ions alone. TOC was determined using a TOC meter on filtrates obtained by centrifugation at 4000 rpm and through 0.45 μm PES membranes.

2.7. Stepwise Inhibition of Metabolism in AnGS under HA Stress

This study utilized four different substrate matrices and pre-existing domesticated granular sludge (Section 2.1) to conduct a methanogenic-capacity experiment. This experiment was conducted to identify the key step inhibiting the anaerobic digestion process. The only carbon sources utilized in the batch tests were starch, casein, glucose, and crystalline sodium acetate. Except for the crystallized sodium acetate group, which had a COD of 2000 mg/L, the simulated wastewater in the other groups had a COD of 8000 mg/L. These concentrations were used to prevent excessive acidification from interfering with the normal anaerobic digestion process. The simulated wastewater from the HA, HA–Ca, and CA groups received an additional 3 g/L of HAs, 3 g/L of HAs with a 200-mg/L Ca ion solution, and a 200 mg/L Ca ion solution, respectively. The domesticated granular sludge was placed into 250 mL fermentation flasks in duplicate to run a reaction, with the entire process being conducted at 35 ± 0.5 °C and 80 rpm. After 1–3 d of the reaction, samples were collected to reflect the actual gas production situation. They were passed through a 0.45 μm PES membrane filter to measure the COD, pH, VFA content, and other standard indicators.

To determine the influence of HAs on methane yield and the time characteristics of gas production, methane production was fitted using the modified Gompertz model. The model is represented as shown in Equation (1):

$$M(t) = M_0 \times exp\left\{1 - exp\left[\frac{R_m \times e}{M_0}(\lambda - t)\right]\right\} \tag{1}$$

where M(t) is the cumulative total methane production (mL/g VSS), M_0 is the final methane production potential (mL/g VSS), and R_m is the maximum methane production rate (mL/g

VSS/h). *e* is Euler's constant (2.71828) and λ is the duration of the lag phase (h), or the minimum amount of time needed to produce methane gas (h).

2.8. Key Enzymatic Activity Tests

To determine the mechanisms through which HAs and Ca ions impact the hydrolysis of anaerobic digestion, the enzymatic activities of hydrolytic enzymes (alkaline protease [AP] and α-glucosidase [α-GC]) in three different forms—free, floc-bound, and granule-bound—were measured.

2.8.1. Alkaline Protease

Alkaline Protease (AP, activity level of 200 U/mL) was acquired from Maclean and subsequently diluted to a concentration of 15 U/mL. The AP activity was evaluated per the literature [44,45] as follows:

$$X_i = \frac{(C - C_0) \times V \times N}{V_0 \times T} \tag{2}$$

where C and C_0 represent the tyrosine concentrations in the experimental and control groups, respectively. V is the total volume of the enzyme reaction system, V_0 is the amount of enzyme involved in the reaction, T is the reaction time, and the enzymatic activity is expressed in the unit of U/mL.

2.8.2. α-glucosidase

The activity of α-glucosidase (α-GC) was measured using an α-GC kit (Suzhou Grace Biotechnology Co., Ltd., Suzhou, China). For this experiment, each gram of VSS sludge sample producing 1 nmol of para-nitrophenol per minute was defined as one unit of enzymatic activity (nmol·min^{-1}·(gVSS)$^{-1}$). The formula is shown in Equation (3):

$$X_{\alpha-GC} = \left[\frac{(\Delta A - 0.1272)}{0.6548}\right] / (W \times V \times T) \tag{3}$$

where ΔA is the difference in absorbance between the assay and control tubes. W is the sample mass (g), V is the volume of the sample introduced into the reaction system (mL), and T is the reaction time (min).

3. Results and Discussion

3.1. Methanogenic Potential Inhibition

The use of simulated carbon sources (starch, casein, glucose, and sodium acetate) facilitates the elucidation of the influence of HAs on three elementary anaerobic digestion reactions: hydrolysis, acidogenesis, and methanogenesis. The fully acidified substrate (FAS) group consisted of a glucose medium and a sodium acetate medium, while the partially acidified substrate (PAS) group consisted of a starch medium and a casein medium.

Figure 1a,c demonstrate that HAs have a considerable inhibitory effect on methane production. In the PAS group, methane production decreased by 11% and 26%, respectively, compared to that in the control group. Enzymes responsible for hydrolysis and their metabolic activities are primarily found in the extracellular region [46]. Therefore, before involvement in the subsequent anaerobic digestion process, the substrates of the PAS group must undergo hydrolysis and transformation into smaller molecules. The inhibition of hydrolysis by HAs delayed acidification and methanation (Figure 1a–d). The accumulation of acetic acid in the VFAs (Figure 1b) indicated that were was no considerable alteration of methane production in the starch. However, the HAs inhibited methanation, while the acetic acid content increased by 232.23 mg/L. The cumulative methane generation in the HA–Ca group increased significantly by approximately 50 mL, whereas the VFA content decreased slightly compared to that in the HA group. This suggests that the bridging interaction of Ca ions with HAs [47] can alleviate the inhibitory effect of methanation. In the

FAS group, methane and VFA production varied minimally (18.11 mg/L and 3.36 mg/L for glucose and sodium acetate, respectively), indicating that HAs exerted a limited influence on the acidification and methanation stages. The results of adjusting the cumulative methane production data to the modified Gompertz model [48,49] are shown in Table 1. The fitting results of the PAS group indicated that the HA group had a lower maximal methane production rate than the control group, with the two groups showing values of 0.22 and 1.01 mL/g VSS/h, respectively. Furthermore, HAs had a minor negative influence on the methane production rate. When comparing the lag phase (λ, time taken for microbial adaptation to substrates and beginning of biomethane production [50]) results, it was observed that the experimental groups containing HAs in the starch group had a shorter lag phase compared to that of the control group (3.65, 5.46 h). This suggests that HAs had a more significant inhibitory effect on the hydrolysis stage of the anaerobic digestion of starch substrates.
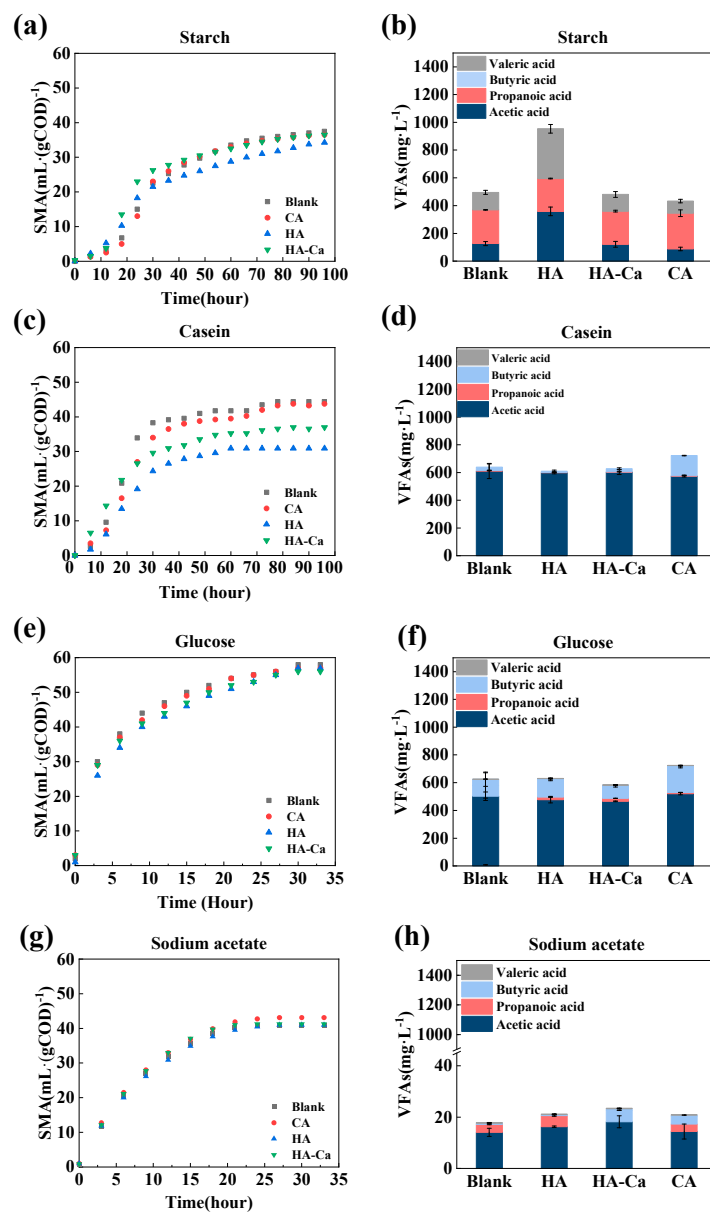
Figure 1. Methane and volatile fatty acids (VFAs) production in PAS and FAS groups. Production of methane: (**a**) starch, (**c**) casein, (**e**) glucose, and (**g**) sodium acetate; production of VFAs: (**b**) starch, (**d**) casein, (**f**) glucose, and (**h**) sodium acetate.

Table 1. Biochemical methane potential and parameters of mathematical adjustments (modified Gompertz) obtained under different conditions.

Substrate Type	Group	M_0 (mL/g VSS)	R_m (mL/g VSS/h)	λ (h)	R^2
Starch	S-Blank	36.53 ± 0.10	0.97 ± 0.01	23.05 ± 0.12	0.993
	S-Ca	35.21 ± 0.10	1.17 ± 0.02	23.53 ± 0.12	0.992
	S-HAs	32.54 ± 0.15	0.75 ± 0.01	19.40 ± 0.20	0.981
	S-HA–Ca	34.32 ± 0.13	1.22 ± 0.03	17.59 ± 0.18	0.978
Casein	C-Blank	42.33 ± 0.10	2.12 ± 0.03	14.79 ± 0.09	0.992
	C-Ca	41.30 ± 0.11	1.60 ± 0.02	16.55 ± 0.10	0.992
	C-HAs	30.74 ± 0.04	1.11 ± 0.01	16.49 ± 0.05	0.998
	C-HA–Ca	35.53 ± 0.08	1.19 ± 0.01	11.26 ± 0.10	0.992
Glucose	G-Blank	57.46 ± 0.17	3.48 ± 0.09	1.45 ± 0.12	0.969
	G-Ca	56.70 ± 0.15	3.28 ± 0.07	1.43 ± 0.12	0.974
	G-HAs	56.92 ± 0.18	2.76 ± 0.06	1.97 ± 0.13	0.975
	G-HA–Ca	55.83 ± 0.16	2.96 ± 0.07	1.08 ± 0.13	0.972
Sodium acetate	SA-Blank	41.29 ± 0.17	2.91 ± 0.04	4.43 ± 0.06	0.995
	SA-Ca	43.52 ± 0.18	2.89 ± 0.04	4.45 ± 0.05	0.995
	SA-HAs	41.46 ± 0.17	2.67 ± 0.04	4.59 ± 0.05	0.996
	SA-HA–Ca	41.87 ± 0.13	3.07 ± 0.04	4.36 ± 0.04	0.997

Although HAs did not influence the methanogenic performance of the FAS group, they negatively influenced both methanogenic kinetics and methane generation in the PAS group. It is inferred that the possible mechanisms by which HAs inhibited substrate methanation in the PAS group included changes in the occurrence forms of the substrates or reductions in extracellular enzymatic activity [51–53].

3.2. Substrate and Enzyme

3.2.1. Substrate Aggregation

The zeta potential and average particle size of the substrate solutions were measured to determine the impact of HAs and Ca ions on the morphology of the fermentation substrates (casein and starch). The effects of HAs and Ca ions on the solubility or filterability of the substrates were quantified by determining the influence of filtration and centrifugation on the substrates in the solution (in terms of TOC). The findings indicated that starch and casein showed distinct response patterns to HAs and Ca ions during the experiment.

HA addition increased the electrostatic repulsive force between starch particles from −14.3 mV to −24.2 mV. The average particle size of starch decreased from 9.06 μm to 0.54 μm. Hence, filtration and centrifugation did not significantly reduce the starch content of the substrate solutions. Xu et al. [54] suggested that starch is a strong competitor of enzymes for binding Ca ions. Therefore, the addition of Ca ions effectively bound to starch resulted in a 4.89 μm increase in particle size of starch in the HA-Ca group compared to the HA group, and counteracted the negative charge from −24.17 mV to −8.41 mV of the starch granules, and reduced the dispersion of HAs on the starch granules [55]. The increase in negative charge due to the addition of HAs suggested that HAs may reduce the contact probability between substrate and enzyme by increasing the electrostatic repulsion force between substrate and hydrolysis, which in turn, reduces the efficiency of hydrolytic enzymes in degrading the substrate, ultimately showing an inhibited anaerobic digestion efficiency. The average size of the starch particles increased significantly from 0.54 μm to 8.17 μm in the HA group (Figure 2c). Of note, the addition of Ca ions to the simulated wastewater impacted the size of the starch particles. However, the Ca ions substantially

reduced the amount of starch in the liquid phase (supernatant or filtrate) after filtration and centrifugation, as shown in Figure 2e.
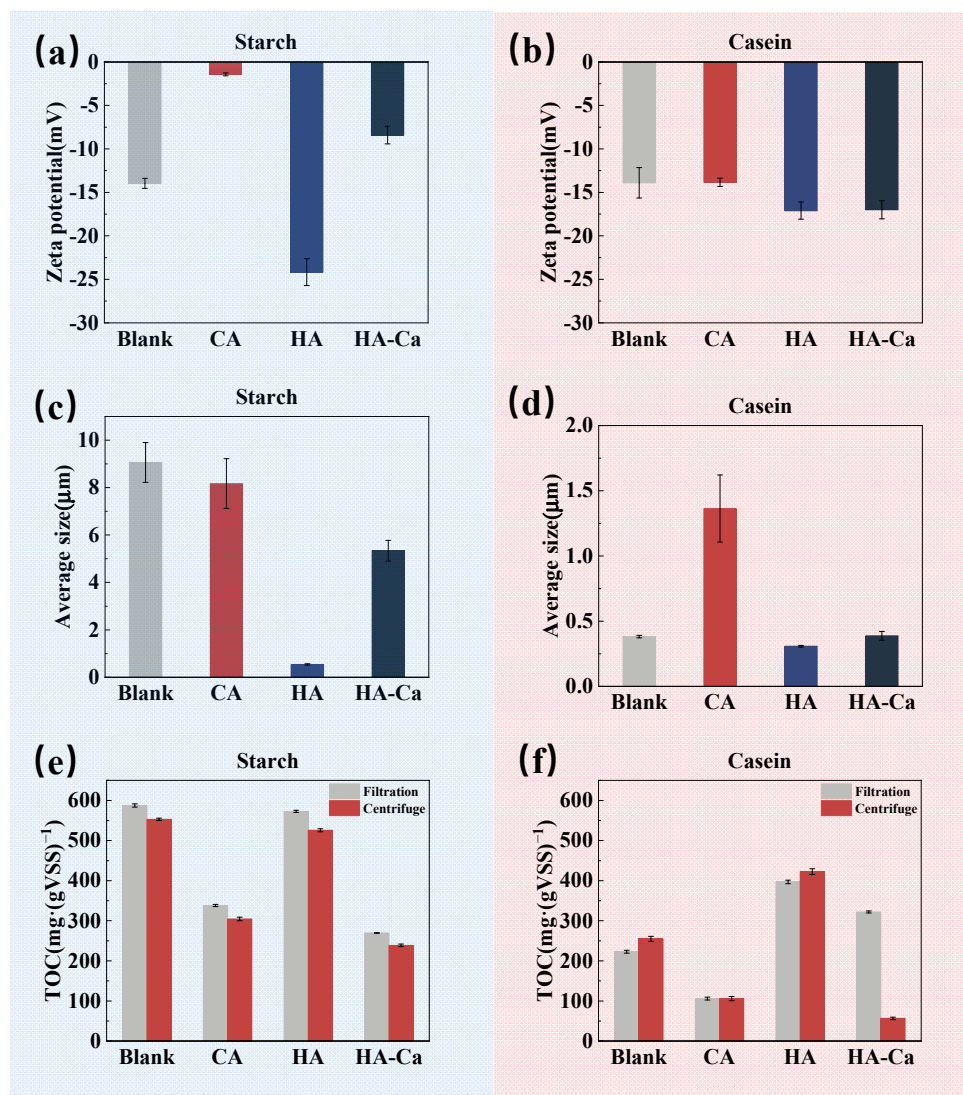

Figure 2. Changes in aggregation state of FAS group substrates under the influence of HAs and Ca ions. (**a**,**b**) Zeta potential of starch and casein under the influence of HAs and Ca ions; (**c**,**d**) particle sizes of starch and casein under the influence of HAs and Ca ions; (**e**,**f**) TOC of starch and casein after filtration and centrifugation.

HA addition did not significantly impact the zeta potential of casein dispersion (Figure 2b). In addition, the particle size of casein remained the same as that of the blank group in the presence of HAs and HA–Ca (Figure 2d). The TOC concentration of the filtrate and centrifugation supernatant in the HA group (174.02 mg/g VSS) was higher than that in the blank group (167.65 mg/g VSS), indicating that the introduction of HAs improved the solubility or dispersion of casein because of the chelation effect of Ca ions with HAs [56]. Differences in the TOC concentration between the centrifugation supernatant and the filtrate, measured at 365.87 mg/g VSS in the HA–Ca group, could be attributed to the increased density of casein colloids following the adsorption of Ca ions. The increased density of casein due to the adsorption of calcium ions made it easier to precipitate during centrifugation, leading to a decrease in the amount of casein in the suspension after centrifugation. This is in agreement with the findings of Sentis-More et al. [57]. Hence, Ca ions enhanced the efficacy of centrifugation in eliminating casein from the HA–Ca group.

3.2.2. Enzymatic Activity

HAs in the PAS group appeared to have a detrimental effect on methanation (as discussed in Section 3.1). It was indicated that HAs may block the breakdown of starch and casein by limiting the activity of extracellular enzymes [58]. Extracellular hydrolases may occur in the effluent of anaerobic reactors, floc sludge, and granular sludge [59]. According to the occurrence forms of enzymes, these hydrolases can be classified as free, floc-bound, or granule-bound enzymes. This section explores the significance of the occurrence form of enzymes as it relates to the inhibitory effect of HAs on enzymatic activity, with α-GC and AP used as specific examples.

According to Figure 3, the activity of free enzymes (α-GC) was measured to be 0.55 nmol /min/gVSS. The HAs significantly decreased the activity of free enzymes by 79.96% and 73.79% for the HA and HA–Ca groups, respectively. HAs can modify the configuration of α-GC active sites [60]. Alternatively, HAs may compete with the substrates, thereby decreasing the probability of the substrates binding to the active sites of the enzymes. This, in turn, may decrease the enzymatic activity [46,61]. HAs increased the electrostatic repulsive force among starch granules, leading to a significant reduction of 93% in the particle size (Figure 2c,d). This permitted the absorption of a more significant amount of enzymes by the starch granules, which then accelerated the process of starch hydrolysis.
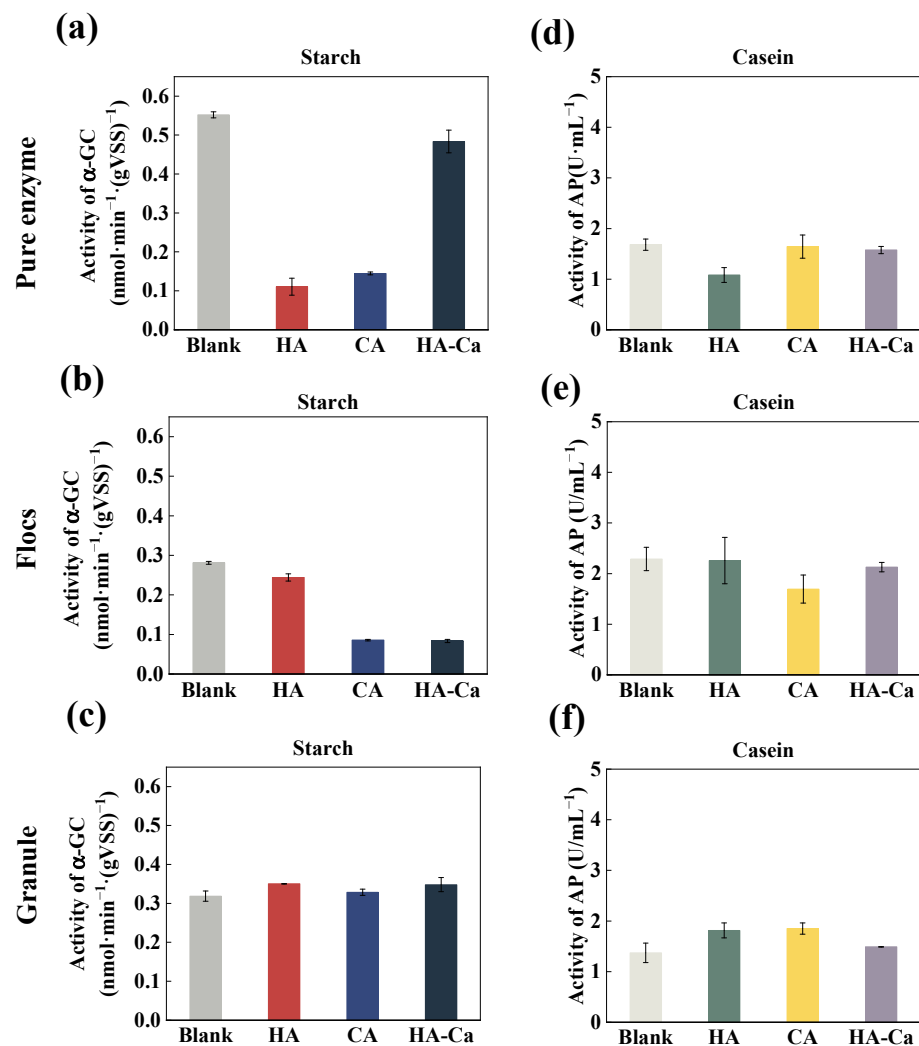
Figure 3. Changes in enzymatic activities in different fugitive states under the influence of HAs and Ca ions (pure enzymes, flocs, granules). (**a**–**c**) a-glucosidase (a-GC) and (**d**–**f**) alkaline protease (AP).

Diffusion is necessary for reciprocal interactions and the attachment of both HAs and enzymes [62]. In contrast to free enzymes, floc-bound and granule-bound enzymes are located within the sludge. HAs must permeate from the bulk liquid into sludge flocs or particles to attach to enzymes. A larger sludge size increases the distance required for mass transfer [63] and the EPSs of sludge adsorbed HAs, thus decelerating the diffusion of HAs into the interior of the sludge. The results demonstrated that floc-bound and granule-bound enzymes effectively protect the activity of α-GC under the influence of HAs. However, the activity of α-GC and AP in the granular-bound enzymes remained unaffected by HAs (0.24 nmol/min/gVSS, 2.26 U/mL) as the large specific surface area of flocculated sludge allowed it to compete with extracellular enzymes for adsorption of HAs [64]. Consequently, the inhibitory effect of HAs on extracellular enzymes was eliminated. Ca ion addition to the starch solution decreased the activity of the enzyme. Ca ions play a crucial role in the formation of floc sludge. By increasing the concentration of Ca ion, the electrostatic repulsive force between small flocs can be reduced, thus increasing the size of the floc particles [65]. The increased size of the floc and granule sludge creates a greater distance between the enzyme and the water phase, making it more difficult for the substrate to be transferred [66]. Consequently, the rate of the enzymatic process within the floc appeared to be slow (0.086 nmol/min/gVSS, 1.69 U/mL).

In summary, the activity of free hydrolases was significantly hindered by HAs, whereas that of hydrolases within flocs and granular sludge was less influenced by HAs. Hence, the decreased methanogenic activity observed in the PAS group under HA stress could be attributed to the ineffective binding of HAs to hydrolytic enzymes, which reduced the efficiency of generating and delivering intermediates, such as VFAs. Consequently, the scarcity of available substrates impeded the growth and activity of methanogenic bacteria.

3.3. Assessment of Potential Impacts on Microbial Aggregation

The median diameter (D50) is a metric used to quantify the physical attributes of particles and precisely indicates the homogeneity of the particles [67–69]. D10 and D90 mean the particle size of a sample when the cumulative size distribution reaches 10% and 90%, respectively. Figure 4a–c display the particle size distribution of the flocculated sludge under HA stress that lasted for 60 h. In the blank group, the flocculated sludge showed a gradual stabilization in its size distribution after 60 h, with a D50 concentration in the 25–35 μm range. Despite undergoing ultrasonication, the granular sludge retained its flocculation ability, whereby small flocs gradually aggregated to form larger floc structures [70]. In HA group, the D50 values were 0.04, 1.44, 4.47, 7.87, and 7.94 μm lower than those in the control group, respectively. HAs inhibited the regeneration of sludge flocs, thereby hindering the aggregation of smaller flocs into larger flocs and resulting in a more dispersed sludge system [71]. Studies [72] have revealed that floc size is related to sludge flocculation. The D50 of the HA–Ca group remained within the range of 13–16 μm, consistently lower than that of the HA group by 0, 4.3, 2.2, 13.3, and 14.8 μm, respectively, which indicated a relatively uniform particle size distribution [73,74]. Cui et al. [75] observed that Ca ions could bind EPSs to accelerate the formation of granules. Although the introduction of Ca ions did not alleviate the inhibitory effect of HAs on floc regeneration, it contributed to greater stability within the flocs [76]. Therefore, it can be concluded that HAs inhibit the aggregation and regeneration of sludge flocs, thus representing an important factor hindering the granulation of sludge particles.

Zeta potential was analyzed for both granular and flocculated sludge to elucidate the variability in the distribution of sludge particle sizes (Figure 5a,b). The sludge particles frequently displayed an electrostatic repulsive force within the range of −10 to −25 mV. Furthermore, the zeta potential of pure HAs is approximately −40 mV, which effectively decreases the surface and interfacial tension of water [77,78]. Figure 5a demonstrates that the zeta potential of the flocs in the HA group decreased by 17.41 mV after 1 h compared to that in the blank group. The introduction of HAs also decreased the zeta potential in the granular sludge. The zeta potentials of the flocs and granular sludge increased by

approximately 2.89–17.31 mV and 3.57–16.31 mV in the HA–Ca group, respectively. HAs augmented the electrostatic repulsive force between the floc sludge particles [79]. The changes in electrostatic repulsion, coupled with the reduced particle size observed in the HA group of Section 3.1 in the article, suggested that the HAs promoted greater dispersion between sludge particles. Moreover, the HAs weakened the ability of flocculation of the flocs [80]. Ding et al. [81] and Yousefi et al. [82] found that a heightened electrostatic repulsive force between sludge particles and a diminished flocculation capability impeded the granulation of sludge, potentially resulting in a tendency towards sludge disintegration and subsequent biomass loss within anaerobic digestion reactors. Moreover, Ca ions can undergo complexation with HAs to alleviate this situation. Consequently, the HAs showed a negative influence on the granularity of sludge, which led to reduced biomass and the inefficiency of anaerobic digestion, ultimately resulting in abnormal operation of the anaerobic digestion reactor.
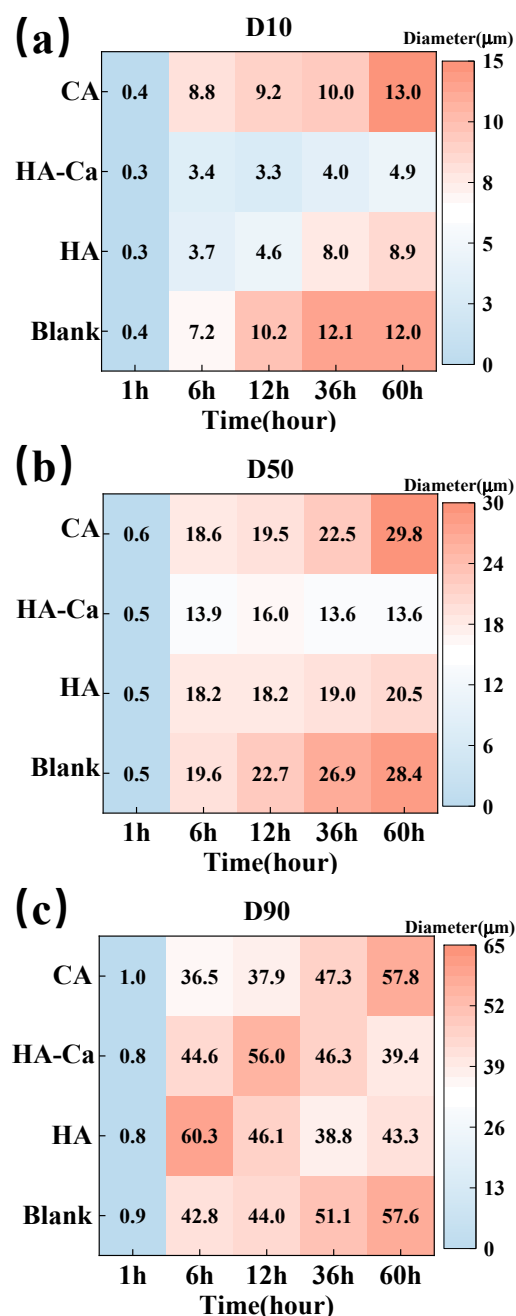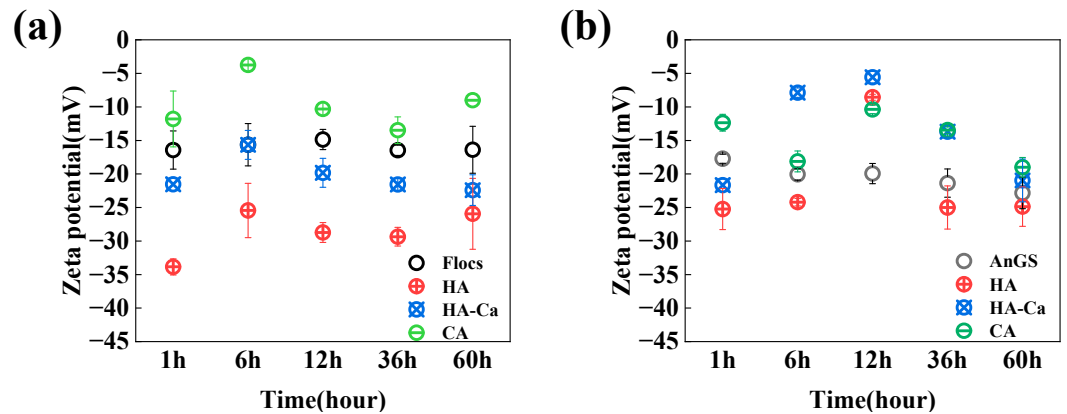

Figure 4. Heat map of particle size distribution of flocculated sludge. (**a**) D10; (**b**) D50; and (**c**) D90.
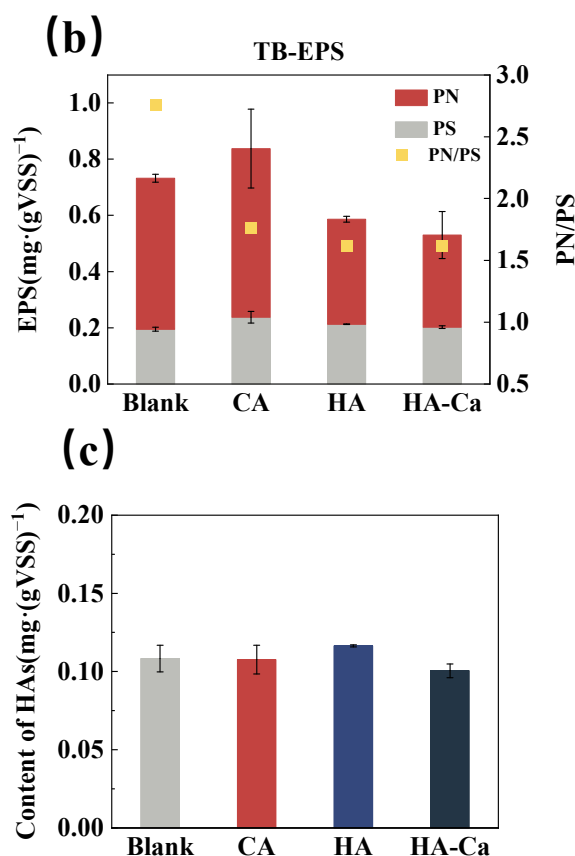
Figure 5. Effect of HAs and Ca ions on zeta potential of flocculated sludge and granular sludge. (**a**) Flocs, (**b**) Aneaerobic granule sludge.

EPSs are the primary components of microbial aggregates and play crucial roles in various aspects of sludge, such as structure, surface charge, flocculation, settling capabilities, and dewatering properties [83–85]. Figure 6a,b illustrate the variations in the contents of LB-EPS and TB-EPS. The content of LB-EPS and the proportions of PNs and PSs change minimally. The inclusion of HAs resulted in a 30.45% reduction in the PN content and a 9.10% increase in the PS, as reflected by the TB-EPS content. PNs, a crucial component of EPSs, supply energy to and safeguard microorganisms engaged in different metabolic processes within the EPSs [86]. Therefore, the reduced PN content caused by the HAs led to an inhibition of the physiological and metabolic activities of microorganisms involved in extracellular hydrolysis and acidification. In addition, the abundance of positively charged amino groups in the PNs counterbalanced the negative charges associated with the carboxyl and phosphate groups [87]. The impact of the EPS proportion on microbial flocculation has been emphasized in previous studies [88–90]. Ding et al. [91] and Jiang et al. [92] proposed that the flocculation capacity and sludge volume index of sludge correlate negatively with the PN/PS ratio. Therefore, the 41.30% decrease in the PN/PS ratio of the HA group suggested that HAs blocked the production of sludge particles and negatively impacted the settling performance of the sludge [93]. In the CA group, the PN content exceeded that of the control group, which demonstrated that moderate concentrations of Ca ions can enhance the release of EPSs from granular sludge and promote their interaction with EPSs to enhance the aggregation of microbial clusters [94]. It can be concluded that HAs adversely influenced the flocculation ability of the sludge and resulted in sludge disintegration and impeded sludge granulation.
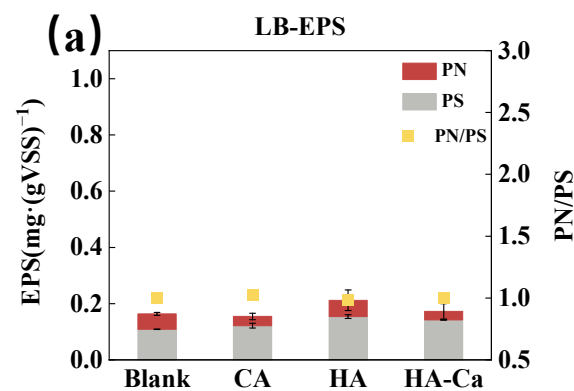
Figure 6. *Cont.*

Figure 6. Effect of HAs and Ca ions on the change in EPS content of sludge and HA content in EPSs. (**a**) LB-EPS; (**b**) TB-EPS; and (**c**) HA content.

4. Conclusions

This study employed HAs as a model substance representing lignin derivatives to investigate the potential influences of simulated CTMP wastewater on the functionality and structural integrity of AnGS. Moreover, the role of coexisting Ca ions was analyzed. The conclusions are as follows: First, the hydrolysis degree of substrates was directly correlated with the inhibitory effects of HAs on anaerobic digestion. HAs hindered the hydrolysis of organic macromolecules in wastewater by suppressing the activity of extracellular enzymes (α-GC and AP), consequently inhibiting the methanogenic activity in the AnGS. Second, the reduced contents of PN in EPS and the increased floc-to-floc electrostatic repulsive force of granular sludge in wastewater containing HAs, along with the increased floc electrostatic repulsive force, indicate that HAs are potential factors inducing granular sludge disintegration or inhibiting sludge granulation. Last, Ca ions did not significantly influence the activity of extracellular enzymes. However, they could reduce the electrostatic repulsive force among sludge particles, thus preserving the stability of the granular sludge structure.

The studies cited indicated that lignin derivatives found in pulping wastewater can have detrimental effects on AnGS reactors in two manners: first, by impeding methanogenic processes through the inhibition of extracellular enzymatic activity, and then by causing a loss of biomass due to hindered sludge granulation. Therefore, in the treatment of pulp and paper industry wastewater, we should reduce the generation of lignin derivatives or avoid the reduction of hydrolase activity during anaerobic digestion by pretreatment. At the same time, the complexation of lignin derivatives by Ca ions may be able to alleviate the inhibition of lignin derivatives in anaerobic digestion. It is necessary to further investigate the effect of Ca ions on reducing the inhibition of lignin derivatives in actual industrial production.

References

1. Lin, C.; Wu, P.; Liu, Y.; Wong, J.W.; Yong, X.; Wu, X.; Zhou, J. Enhanced biogas production and biodegradation of phenanthrene in wastewater sludge treated anaerobic digestion reactors fitted with a bioelectrode system. *Chem. Eng. J.* **2019**, *365*, 1–9. [CrossRef]
2. Singh, A.K.; Chandra, R. Pollutants released from the pulp paper industry: Aquatic toxicity and their health hazards. *Aquat. Toxicol.* **2019**, *211*, 202–216. [CrossRef]
3. Lappalainen, J.; Baudouin, D.; Hornung, U.; Schuler, J.; Melin, K.; Bjelić, S.; Joronen, T. Sub- and Supercritical Water Liquefaction of Kraft Lignin and Black Liquor Derived Lignin. *Energies* **2020**, *13*, 3309. [CrossRef]
4. Pokhrel, D.; Viraraghavan, T. Treatment of pulp and paper mill wastewater—A review. *Sci. Total Environ.* **2004**, *333*, 37–58. [CrossRef]
5. Martin, N.; Anglani, N.; Einstein, D.; Khrushch, M.; Worrell, E.; Price, L.K. Opportunities to Improve Energy Efficiency and Reduce Greenhouse Gas Emissions in the U.S. Pulp and Paper Industry. 2000. 56p. Available online: https://escholarship.org/content/qt31b2f7bd/qt31b2f7bd.pdf (accessed on 7 April 2024).
6. Kumar, V.; Thakur, I.S.; Shah, M.P. Bioremediation Approaches for Treatment of Pulp and Paper Industry Wastewater: Recent Advances and Challenges. In *Microbial Bioremediation & Biodegradation*; Shah, M.P., Ed.; Springer: Singapore, 2020; pp. 1–48.
7. Hermosilla, D.; Merayo, N.; Gascó, A.; Blanco, Á. The application of advanced oxidation technologies to the treatment of effluents from the pulp and paper industry: A review. *Environ. Sci. Pollut. Res. Int.* **2015**, *22*, 168–191. [CrossRef]
8. Zainith, S.; Chowdhary, P.; Bharagava, R.N. Recent Advances in Physico-chemical and Biological Techniques for the Management of Pulp and Paper Mill Waste. In *Emerging and Eco-Friendly Approaches for Waste Management*; Bharagava, R.N., Chowdhary, P., Eds.; Springer: Singapore, 2019; pp. 271–297.
9. Ramesh, S.; Chaurasia, A.S.; Mahalingam, H.; Rao, N.J. Kinetics of Devolatilization of Black Liquor Droplets in Chemical Recovery Boilers—Pyrolysis of Dry Black Liquor Solids. *Int. J. Chem. Eng. Appl.* **2013**, *4*, 1–5. [CrossRef]
10. Jian, Z.; Yuan-Fang, P.; Wan-Li, W.; Qin, W.; Gong-Nan, X.; Hong-Fei, L.; Tian, X.; Shuang-Fei, W. Black liquor increases methane production from excess pulp and paper industry sludge. *Chemosphere* **2021**, *280*, 130665. [CrossRef]
11. Welander, T. An Anaerobic Process for Treatment of CTMP Effluent. *Water Sci. Technol.* **1988**, *20*, 143–147. [CrossRef]
12. Kudo, A.; Kennedy, K.; Andras, E. Anaerobic (UASB) Treatment of Pulp (CTMP) Wastewater and the Toxicity on Granules. *Water Sci. Technol.* **1991**, *23*, 1919–1928. [CrossRef]
13. Pathak, P.; Sharma, C. Processes and problems of pulp and paper industry: An overview. *Phys. Sci. Rev.* **2023**, *8*, 299–325. [CrossRef]
14. Ho, D.P.; Ngo, H.H.; Guo, W. A mini review on renewable sources for biofuel. *Bioresour. Technol.* **2014**, *169*, 742–749. [CrossRef]
15. Kumar, S.; Haq, I.; Yadav, A.; Prakash, J.; Raj, A. Immobilization and Biochemical Properties of Purified Xylanase from Bacillus amyloliquefaciens SK-3 and Its Application in Kraft Pulp Biobleaching. *J. Clin. Microbiol. Biochem. Technol.* **2016**, *2*, 26–34.
16. Fang, X.; Li, Q.; Lin, Y.; Lin, X.; Dai, Y.; Guo, Z.; Pan, D. Screening of a microbial consortium for selective degradation of lignin from tree trimmings. *Bioresour. Technol.* **2018**, *254*, 247–255. [CrossRef]
17. Sun, J.; Li, H.; Xiao, L.-P.; Guo, X.; Fang, Y.; Sun, R.-C.; Song, G. Fragmentation of Woody Lignocellulose into Primary Monolignols and Their Derivatives. *ACS Sustain. Chem. Eng.* **2019**, *7*, 4666–4674. [CrossRef]
18. Yu, J.; Wang, D.; Sun, L. The pyrolysis of lignin: Pathway and interaction studies. *Fuel* **2021**, *290*, 120078. [CrossRef]
19. Balasundaram, G.; Banu, R.; Varjani, S.; Kazmi, A.; Tyagi, V.K. Recalcitrant compounds formation, their toxicity, and mitigation: Key issues in biomass pretreatment and anaerobic digestion. *Chemosphere* **2022**, *291 Pt 3*, 132930. [CrossRef]
20. Li, W.; Khalid, H.; Zhu, Z.; Zhang, R.; Liu, G.; Chen, C.; Thorin, E. Methane production through anaerobic digestion: Participation and digestion characteristics of cellulose, hemicellulose and lignin. *Appl. Energy* **2018**, *226*, 1219–1228. [CrossRef]
21. Koyama, M.; Yamamoto, S.; Ishikawa, K.; Ban, S.; Toda, T. Inhibition of anaerobic digestion by dissolved lignin derived from alkaline pre-treatment of an aquatic macrophyte. *Chem. Eng. J.* **2017**, *311*, 55–62. [CrossRef]

22. Shad, M.; Nazir, A.; Usman, M.; Akhtar, M.W.; Sajjad, M. Investigating the effect of SUMO fusion on solubility and stability of amylase-catalytic domain from *Pyrococcus abyssi*. *Int. J. Biol. Macromol.* **2024**, *266 Pt 2*, 131310. [CrossRef] [PubMed]

23. de Souza, D.; Sbardelotto, A.F.; Ziegler DD, R.; Pinto LM, N.; de Souza Ramos, R.C.; Marczak LD, F.; Tessaro, I.C. Obtaining and purification of a highly soluble hydrolyzed rice endosperm protein. *Sep. Purif. Technol.* **2017**, *183*, 279–292. [CrossRef]

24. Li, B.; Xie, Y.; Guo, Q. Thermal acid hydrolysis modulates the solubility of quinoa protein: The formation of different types of protein aggregates. *Food Hydrocoll.* **2024**, *151*, 109825. [CrossRef]

25. Priya; Gogate, P.R. Ultrasound-Assisted Intensification of Activity of Free and Immobilized Enzymes: A Review. *Ind. Eng. Chem. Res.* **2021**, *60*, 9650–9668. [CrossRef]

26. Bernardes, A.; Pellegrini, V.; Curtolo, F.; Camilo, C.; Mello, B.; Johns, M.; Scott, J.; Guimaraes, F.; Polikarpov, I. Carbohydrate binding modules enhance cellulose enzymatic hydrolysis by increasing access of cellulases to the substrate. *Carbohydr. Polym.* **2019**, *211*, 57–68. [CrossRef]

27. Li, J.; Hao, X.; van Loosdrecht, M.C.; Liu, R. Relieving the inhibition of humic acid on anaerobic digestion of excess sludge by metal ions. *Water Res.* **2021**, *188*, 116541. [CrossRef] [PubMed]

28. El Ouaqoudi, F.Z.; Meddich, A.; Lemée, L.; Amblès, A.; Hafidi, M. Assessment of Compost-Derived Humic Acids Structure from Ligno-Cellulose Waste by TMAH-Thermochemolysis. *Waste Biomass Valorization* **2018**, *10*, 2661–2672. [CrossRef]

29. Norrman, J.; Narbuvold, R. Anaerobic Treatability of Waste Waters from Pulp and Paper Industries. *Biotechnol. Adv.* **1984**, *2*, 329–345. [CrossRef] [PubMed]

30. Noike, T.; Endo, G.; Chang, J.; Yaguchi, J.; Matsumoto, J. Characteristics of Carbohydrate Degradation and the Rate-limiting Step in Anaerobic Digestion. *Biotechnol. Bioeng.* **1985**, *27*, 1482–1489. [CrossRef] [PubMed]

31. Xu, Y.; Lu, Y.; Zheng, L.; Wang, Z.; Dai, X. Effects of humic matter on the anaerobic digestion of sewage sludge: New insights from sludge structure. *Chemosphere* **2020**, *243*, 125421. [CrossRef] [PubMed]

32. Azman, S.; Khadem, A.F.; Plugge, C.M.; Stams, A.J.M.; Bec, S.; Zeeman, G. Effect of humic acid on anaerobic digestion of cellulose and xylan in completely stirred tank reactors: Inhibitory effect, mitigation of the inhibition and the dynamics of the microbial communities. *Appl. Microbiol. Biotechnol.* **2017**, *101*, 889–901. [CrossRef]

33. Li, J.; Hao, X.; van Loosdrecht, M.C.; Yu, J.; Liu, R. Adaptation of semi-continuous anaerobic sludge digestion to humic acids. *Water Res.* **2019**, *161*, 329–334. [CrossRef]

34. Batstone, D.; Landelli, J.; Saunders, A.; Webb, R.; Blackall, L.; Keller, J. The influence of calcium on granular sludge in a full-scale UASB treating paper mill wastewater. *Water Sci. Technol.* **2002**, *45*, 187–193. [CrossRef] [PubMed]

35. Vegunta, V.; Sevastyanova, O.; Deshpande, R.; Lindén, P.A.; Garcia, A.; Björk, M.; Jansson, U.; Henriksson, G.; Lindström, M.E. Addition of green and black liquor in kraft pulping of Eucalyptus dunnii wood: Possible solutions for the problems with kraft pulping caused by high calcium content. *Cellulose* **2023**, *31*, 1223–1236. [CrossRef]

36. Schneider, T.; Roffael, E.; Dix, B. Einfluß von Holzaufschlußverfahren (TMP-, CTMP-Verfahren) und Aufschlußbedingungen auf die physikalisch-technologischen Eigenschaften von mitteldichten Faserplatten (MDF). *Eur. J. Wood Wood Prod.* **2000**, *58*, 123–124. [CrossRef]

37. Hering, J.G.; Morel, F.M. Humic acid complexation of calciun and copper. *Environ. Sci. Technol.* **1988**, *22*, 1234–1237. [CrossRef] [PubMed]

38. Christl, I. Ionic strength- and pH-dependence of calcium binding by terrestrial humic acids. *Environ. Chem.* **2012**, *9*, 89–96. [CrossRef]

39. Lin, L.; Ishida, K.; Zhang, Y.; Usui, N.; Miyake, A.; Abe, N.; Li, Y.-Y. Improving the biomass retention and system stability of the anammox EGSB reactor by adding a calcium silicate hydrate functional material. *Sci. Total Environ.* **2023**, *857 Pt 3*, 159719. [CrossRef] [PubMed]

40. *CJ/T 221-2005*; Municipal Wastewater Treatment Plant Sludge Inspection Methods. Technical Committee for the Standardisation of Water Supply and Drainage Products of the Ministry of Construction: Beijing, China, 2005.

41. Wang, X.; Zhang, M.; Zhou, Z.; Qu, T.; Ran, J.; Zhang, J.; Li, X.; Zhang, L.; Zhang, A. Effect of extracellular polymeric substances removal and re-addition on anaerobic digestion of waste activated sludge. *J. Water Process Eng.* **2024**, *57*, 108069. [CrossRef]

42. Frølund, B.; Palmgren, R.; Keiding, K.; Nielsen, P.H. Extraction of extracellular polymers from activated sludge using a cation exchange resin. *Water Res.* **1996**, *30*, 1749–1758. [CrossRef]

43. DuBois, M.; Gilles, K.A.; Hamilton, J.K.; Rebers, P.A.; Smith, F. Colorimetric Method for Determination of Sugars and Related Substances. *Anal. Chem.* **1956**, *28*, 350–356. [CrossRef]

44. Goel, R.; Mino, T.; Satoh, H.; Matsuo, T. Enzyme Activities under Anaerobic and Aerobic Conditions in Activated Sludge Sequencing Batch Reactor. *Water Res. A J. Int. Water Assoc.* **1988**, *32*, 2081–2088. [CrossRef]

45. Yan, Y.; Liu, F.; Gao, J.; Wan, J.; Ding, J.; Li, T. Enhancing enzyme activity via low-intensity ultrasound for protein extraction from excess sludge. *Chemosphere* **2022**, *303*, 134936. [CrossRef]

46. Shi, M.; Liu, H.; Zhang, X.; Li, Y.; Huang, F.; Zhao, C.; Liu, H. A neglected contributor of thermal hydrolysis to sludge anaerobic digestion: Fulvic acids release and their influences. *J. Environ. Manag.* **2023**, *343*, 118217. [CrossRef]

47. Dong, H.; Lo, I.M. Influence of calcium ions on the colloidal stability of surface-modified nano zero-valent iron in the absence or presence of humic acid. *Water Res.* **2013**, *47*, 2489–2496. [CrossRef]

48. Karki, R.; Chuenchart, W.; Surendra, K.C.; Sung, S.; Raskin, L.; Khanal, S.K. Anaerobic co-digestion of various organic wastes: Kinetic modeling and synergistic impact evaluation. *Bioresour. Technol.* **2022**, *343*, 126063. [CrossRef]

49. Allen, E.; Wall, D.; Herrmann, C.; Xia, A.; Murphy, J.D. What is the gross energy yield of third generation gaseous biofuel sourced from seaweed? *Energy* **2015**, *81*, 352–360. [CrossRef]

50. Karki, R.; Chuenchart, W.; Surendra, K.; Sung, S.; Raskin, L.; Khanal, S.K. Biogas production from residual marine macroalgae biomass: Kinetic modelling approach. *Bioresour. Technol.* **2022**, *359*, 127473.

51. Takahashi, H.; Li, B.; Sasaki, T.; Miyazaki, C.; Kajino, T.; Inagaki, S. Catalytic Activity in Organic Solvents and Stability of Immobilized Enzymes Depend on the Pore Size and Surface Characteristics of Mesoporous Silica. *Chem. Mater.* **2000**, *12*, 3301–3305. [CrossRef]

52. Huron, M.; Hudebine, D.; Ferreira, N.L.; Lachenal, D. Mechanistic modeling of enzymatic hydrolysis of cellulose integrating substrate morphology and cocktail composition. *Biotechnol. Bioeng.* **2016**, *113*, 1011–1023. [CrossRef]

53. Kumar, R.; Wyman, C.E. Physical and Chemical Features of Pretreated Biomass that Influence Macro-/Micro-Accessibility and Biological Processing. In *Aqueous Pretreatment of Plant Biomass for Biological and Chemical Conversion to Fuels and Chemicals*; Wiley: Hoboken, NJ, USA, 2013; pp. 281–310.

54. Xu, E.; Li, D.; Cheng, H.; Zhao, H.; Tian, J.; Wu, Z.; Chen, S.; Ye, X.; Liu, D. Effect of anion type on enzymatic hydrolysis of starch-(thermostable alpha-amylase)-calcium system in a low-moisture solid microenvironment of bioextrusion. *Carbohydr. Polym.* **2020**, *240*, 116331. [CrossRef]

55. Kraithong, S.; Junejo, S.A.; Jiang, Y.; Zhang, B.; Huang, Q. Effects of pectin-calcium matrices on controlling in vitro digestion of normal maize starch. *Food Hydrocoll.* **2023**, *140*, 108575. [CrossRef]

56. Xu, Y.; Liu, D.; Yang, H.; Zhang, J.; Liu, X.; Regenstein, J.M.; Zhou, P. Effect of calcium sequestration by ion-exchange treatment on the dissociation of casein micelles in model milk protein concentrates. *Food Hydrocoll.* **2016**, *60*, 59–66. [CrossRef]

57. Sentís-Moré, P.; Ortega-Olivé, N.; Mas-Capdevila, A.; Romero-Fabregat, M.-P. Impact of centrifugation and vacuum filtration step on the yield and molecular weight distribution of protein hydrolysates from rapeseed and sunflower meals. *LWT* **2022**, *165*, 113741. [CrossRef]

58. Yap, S.; Astals, S.; Lu, Y.; Peces, M.; Jensen, P.; Batstone, D.; Tait, S. Humic acid inhibition of hydrolysis and methanogenesis with different anaerobic inocula. *Waste Manag.* **2018**, *80*, 130–136. [CrossRef]

59. Ayol, A.; Filibeli, A.; Sir, D.; Kuzyaka, E. Aerobic and anaerobic bioprocessing of activated sludge: Floc disintegration by enzymes. *J. Environ. Sci. Health Part A* **2008**, *43*, 1528–1535. [CrossRef]

60. Ge, X.; Zhang, W.; Putnis, C.V.; Wang, L. Direct observation of humic acid-promoted hydrolysis of phytate through stabilizing a conserved catalytic domain in phytase. *Environ. Sci. Process. Impacts* **2022**, *24*, 1082–1093. [CrossRef]

61. Yu, M.; Zhu, S.; Huang, D.; Tao, X.; Li, Y. Inhibition of starch digestion by phenolic acids with a cinnamic acid backbone: Structural requirements for the inhibition of α-amylase and α-glucosidase. *Food Chem.* **2024**, *435*, 137499. [CrossRef]

62. Zhang, Y.; Hess, H. Enhanced Diffusion of Catalytically Active Enzymes. *ACS Cent. Sci.* **2019**, *5*, 939–948. [CrossRef]

63. Chu, C.P.; Tsai, D.G.; Lee, D.J.; Tay, J.H. Size-dependent anaerobic digestion rates of flocculated activated sludge: Role of intrafloc mass transfer resistance. *J. Environ. Manag.* **2005**, *76*, 239–244. [CrossRef]

64. Tian, S.; Zhu, Y.; Liu, Z.; Zhang, G.; Rao, J.; Li, X. Optimization of low-intensity ultrasonic irradiation for low-strength sewage treatment in anaerobic baffled reactor. *J. Environ. Chem. Eng.* **2022**, *10*, 108022. [CrossRef]

65. He, J.; Zhang, P.; Zou, X.; Zhong, Y.; Pan, X.; Pang, H.; Zhang, J.; Cui, X.; Wu, X.; Li, B.; et al. Impact of divalent cations on lysozyme-induced solubilisation of waste-activated sludge: Perspectives of extracellular polymeric substances and surface electronegativity. *Chemosphere* **2022**, *302*, 134841. [CrossRef]

66. Liu, J.; Xu, Y.; Wei, Y. A model-based approach for evaluating the effects of sludge rheology on methane production during high solid anaerobic digestion: Focusing on mass transfer resistance. *Biochem. Eng. J.* **2024**, *201*, 109147. [CrossRef]

67. Li, Z.; Stenstrom, M.K. Impacts of SRT on Particle Size Distribution and Reactor Performance in Activated Sludge Processes. *Water Environ. Res.* **2018**, *90*, 48–56. [CrossRef]

68. Ward, B.; Nguyen, M.; Sam, S.; Korir, N.; Niwagaba, C.; Morgenroth, E.; Strande, L. Particle size as a driver of dewatering performance and its relationship to stabilization in fecal sludge. *J. Environ. Manag.* **2023**, *326*, 116801. [CrossRef]

69. Abeshu, G.W.; Li, H.-Y.; Zhu, Z.; Tan, Z.; Leung, L.R. Median bed-material sediment particle size across rivers in the contiguous US. *Earth Syst. Sci. Data* **2022**, *14*, 929–942. [CrossRef]

70. Chen, W.; Gao, X.; Xu, H.; Cai, Y.; Cui, J. Influence of extracellular polymeric substances (EPS) treated by combined ultrasound pretreatment and chemical re-flocculation on water treatment sludge settling performance. *Chemosphere* **2017**, *170*, 196–206. [CrossRef]

71. Liu, Q.; Li, Y.; Yang, F.; Liu, X.; Wang, D.; Xu, Q.; Zhang, Y.; Yang, Q. Understanding the mechanism of how anaerobic fermentation deteriorates sludge dewaterability. *Chem. Eng. J.* **2021**, *404*, 127026. [CrossRef]

72. Wu, W.; Zhou, Z.; Chen, L.; Chen, G.; Zhang, Y.; Jiang, L.; Qiu, Z.; He, K.; Wu, Z. Conditioning for excess sludge and ozonized sludge by ferric salt and polyacrylamide: Orthogonal optimization, rheological characteristics and floc properties. *Chem. Eng. J.* **2019**, *373*, 1081–1090. [CrossRef]

73. El Hagrasy, A.S.; Hennenkamp, J.R.; Burke, M.D.; Cartwright, J.J.; Litster, J.D. Twin screw wet granulation: Influence of formulation parameters on granule properties and growth behavior. *Powder Technol.* **2013**, *238*, 108–115. [CrossRef]

74. Mendez Torrecillas, C.; Halbert, G.W.; Lamprou, D.A. A novel methodology to study polymodal particle size distributions produced during continuous wet granulation. *Int. J. Pharm.* **2017**, *519*, 230–239. [CrossRef]

75. Cui, Y.-W.; Huang, J.-L.; Alam, F. Fast granulation of halophilic activated sludge treating low-strength organic saline wastewater via addition of divalent cations. *Chemosphere* **2021**, *264*, 128396. [CrossRef]

76. Feng, L.; Liu, J.; Xu, C.; Lu, W.; Li, D.; Zhao, C.; Liu, B.; Li, X.; Khan, S.; Zheng, H.; et al. Better understanding the polymerization kinetics of ultrasonic-template method and new insight on sludge floc characteristics research. *Sci. Total Environ.* **2019**, *689*, 546–556. [CrossRef] [PubMed]

77. Yang, K.; Yan, X.; Xu, J.; Jiang, L.; Wu, W. Sorption of organic compounds by pyrolyzed humic acids. *Sci. Total Environ.* **2021**, *781*, 146646. [CrossRef] [PubMed]

78. Di Iorio, E.; Circelli, L.; Angelico, R.; Torrent, J.; Tan, W.; Colombo, C. Environmental implications of interaction between humic substances and iron oxide nanoparticles: A review. *Chemosphere* **2022**, *303 Pt 2*, 135172. [CrossRef] [PubMed]

79. Chen, C.; Zhang, T.; Lv, L.; Chen, Y.; Tang, W.; Tang, S. Destroying the structure of extracellular polymeric substance to improve the dewatering performance of waste activated sludge by ionic liquid. *Water Res.* **2021**, *199*, 117161. [CrossRef]

80. Zheng, Y.; Xing, M.; Cai, L.; Xiao, T.; Lu, Y.; Jiang, J. Interaction of earthworms-microbe facilitating biofilm dewaterability performance during wasted activated sludge reduction and stabilization. *Sci. Total Environ.* **2017**, *581–582*, 573–581. [CrossRef]

81. Ding, W.; Jin, W.; Zhou, X.; Yang, Q.; Chen, C.; Wang, Q. Role of extracellular polymeric substances in anaerobic granular sludge: Assessing dewaterability during Fe(II)-peroxydisulfate conditioning and granulation processes. *J. Clean. Prod.* **2021**, *286*, 124968. [CrossRef]

82. Yousefi, S.A.; Nasser, M.S.; Hussein, I.A.; Benamor, A. Enhancement of flocculation and dewaterability of a highly stable activated sludge using a hybrid system of organic coagulants and polyelectrolytes. *J. Water Process Eng.* **2020**, *35*, 101237. [CrossRef]

83. Priyadarshanee, M.; Das, S. Bacterial extracellular polymeric substances: Biosynthesis and interaction with environmental pollutants. *Chemosphere* **2023**, *332*, 138876.

84. An, Q.; Chen, Y.; Tang, M.; Zhao, B.; Deng, S.; Li, Z. The mechanism of extracellular polymeric substances in the formation of activated sludge flocs. *Colloids Surf. A Physicochem. Eng. Asp.* **2023**, *663*, 131009. [CrossRef]

85. Wu, S.; Hua, X.; Miao, R.; Ma, B.; Hu, C.; Liu, H.; Qu, J. Influence of floc charge and related distribution mechanisms of humic substances on ultrafiltration membrane behavior. *J. Membr. Sci.* **2020**, *609*, 118260. [CrossRef]

86. Dong, J.; Zhang, Z.; Yu, Z.; Dai, X.; Xu, X.; Alvarez, P.J.; Zhu, L. Evolution and functional analysis of extracellular polymeric substances during the granulation of aerobic sludge used to treat p-chloroaniline wastewater. *Chem. Eng. J.* **2017**, *330*, 596–604. [CrossRef]

87. Wang, B.-B.; Liu, X.-T.; Chen, J.-M.; Peng, D.-C.; He, F. Composition and functional group characterization of extracellular polymeric substances (EPS) in activated sludge: The impacts of polymerization degree of proteinaceous substrates. *Water Res.* **2018**, *129*, 133–142. [CrossRef] [PubMed]

88. Liu, X.; Liu, J.; Deng, D.; Li, R.; Guo, C.; Ma, J.; Chen, M. Investigation of extracellular polymeric substances (EPS) in four types of sludge: Factors influencing EPS properties and sludge granulation. *J. Water Process Eng.* **2021**, *40*, 101924. [CrossRef]

89. Wan, P.; Liu, Y.; Zhang, Q.; Jiang, L.; Chen, H.; Lv, W. Enhanced degradation of extracellular polymeric substances by yeast in activated sludge to achieve sludge reduction. *Bioresour. Technol.* **2023**, *377*, 128915. [CrossRef] [PubMed]

90. Tang, C.-C.; Zhang, X.; He, Z.-W.; Tian, Y.; Wang, X.C. Role of extracellular polymeric substances on nutrients storage and transfer in algal-bacteria symbiosis sludge system treating wastewater. *Bioresour. Technol.* **2021**, *331*, 125010. [CrossRef] [PubMed]

91. Ding, A.; Lin, W.; Chen, R.; Ngo, H.H.; Zhang, R.; He, X.; Ma, J. Improvement of sludge dewaterability by energy uncoupling combined with chemical re-flocculation: Reconstruction of floc, distribution of extracellular polymeric substances, and structure change of proteins. *Sci. Total Environ.* **2022**, *816*, 151646. [CrossRef] [PubMed]

92. Jiang, B.; Zeng, Q.; Liu, Q.; Chai, H.; Xiang, J.; Li, H.; Shi, S.; Yang, A.; Chen, Z.; Cui, Y.; et al. Impacts of electric field-magnetic powder coupled membrane bioreactor on phenol wastewater treatment: Performance, synergistic mechanism, antibiotic resistance genes, and eco-environmental benefit evaluation. *Sci. Total Environ.* **2024**, *909*, 168607. [CrossRef]

93. Deng, S.; Wang, L.; Su, H. Role and influence of extracellular polymeric substances on the preparation of aerobic granular sludge. *J. Environ. Manag.* **2016**, *173*, 49–54. [CrossRef] [PubMed]

94. Sheng, G.-P.; Xu, J.; Li, W.-H.; Yu, H.-Q. Quantification of the interactions between Ca^{2+}, Hg^{2+} and extracellular polymeric substances (EPS) of sludge. *Chemosphere* **2013**, *93*, 1436–1441. [CrossRef]